

Engineering a Photoactivated Caspase-7 for Rapid Induction of Apoptosis

Evan Mills,[†] Xi Chen,[†] Elizabeth Pham,[†] Stanley Wong,[†] and Kevin Truong^{†,‡,*}

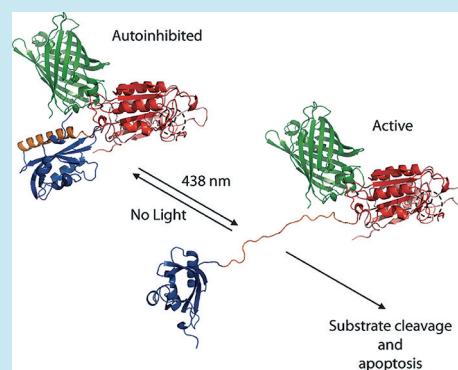
[†]Institute of Biomaterials and Biomedical Engineering, University of Toronto, 164 College Street, Toronto, Ontario M5S 3G9, Canada

[‡]Edward S. Rogers Sr. Department of Electrical and Computer Engineering, University of Toronto, 10 King's College Circle, Toronto, Ontario M5S 3G4, Canada

S Supporting Information

ABSTRACT: Apoptosis is a cell death program involved in the development of multicellular organisms, immunity, and pathologies ranging from cancer to HIV/AIDS. We present an engineered protein that causes rapid apoptosis of targeted cells in monolayer culture after stimulation with blue light. Cells transfected with the protein switch L57V, a tandem fusion of the light-sensing LOV2 domain and the apoptosis-executing domain from caspase-7, rapidly undergo apoptosis within 60 min after light stimulation. Constant illumination of under 5 min or oscillating with 1 min exposure had no effect, suggesting that cells have natural tolerance to a short duration of caspase-7 activity. Furthermore, the overexpression of Bcl-2 prevented L57V-mediated apoptosis, suggesting that although caspase-7 activation is sufficient to start apoptosis, it requires mitochondrial contribution to fully commit.

KEYWORDS: apoptosis, engineered proteins, photoactivatable proteins



Apoptosis is an important programmed cell death pathway in multicellular organisms for processes such as development,¹ cell clearance,^{1,2} and immune response³ and pathologies such as cancer⁴ and HIV/AIDS.⁵ Apoptosis is characterized in the end stages by plasma membrane blebbing and the release of apoptotic bodies, cytoplasmic condensation, and loss of nuclear integrity,⁶ among other biochemical signatures. Apoptosis is usually regulated by a cascade of proteases known as caspases that can respond to intracellular cues (such as caspase-9) or extracellular stimuli (for example, caspase-8).⁷ Upstream, or initiator, caspase activation ultimately results in effector, or executioner, caspase activation, such as caspase-3 or -7. This last check-point in the caspase cascade is an ideal position to develop a control mechanism for cell death because the executioner caspases are responsible for directly carrying out the majority of the apoptosis program.^{7,8} *In vivo* large prodomain-bearing caspases such as caspase-8 and -9 are activated allosterically on platforms (for example, the apoptosome in the case of caspase-9), and the prodomain often mediates the interaction between caspases and modulators of caspase activity.⁷ The smaller caspases such as caspase-3 and -7 are synthesized with short prodomains that are several dozen amino acids in length. Effector caspase activation occurs as a result of homodimerization and internal cleavage into p20 and p10 subunits by upstream caspases.^{6c} This processing is usually accompanied by the removal of the short prodomain, although the causal relationship is not clear given that some

effector caspases, such as caspase-6 can be activated *in vitro* with an intact prodomain.⁹

Light-switchable synthetic proteins are a new class of biochemical tools that are being used to investigate biological interactions and effects with a high degree of spatiotemporal accuracy. These synthetic proteins are usually constructed by a tandem fusion of a light-sensitive domain with the prospective effector domain. A common light-sensitive domain is the LOV2 domain from phototropin1.¹⁰ LOV2 has recently been used to create a photosensitive switch of the small GTPase Rac1,¹¹ the *E. coli* trp repressor¹² and the Ca²⁺ channel Orai1¹³ and has been studied for its potentially generalizable role in photosensitive switches.^{11,14} We thought to use LOV2 as a pseudoprodome for caspase-7 because it exists in a compact form in the dark state and undocks from its J α peptide when illuminated with blue light,¹⁰ thereby exposing whatever is C-terminal to it to other binding partners.

Design of a Photoactivated Caspase-7. A photoactivated caspase could be developed using a pseudoprodome that suppresses the catalytic domain until some signal causes the pseudoprodome to release its autoinhibition and allow the catalytic domain to function as an activated unit. The synthetic protein is a tandem fusion of the LOV2 domain from *A. Sativa* phototropin 1,^{10b} the catalytic domain of caspase-7⁸ from *H. Sapiens*, and the monomeric YFP Venus.¹⁵ Several

Received: September 14, 2011

Published: October 19, 2011



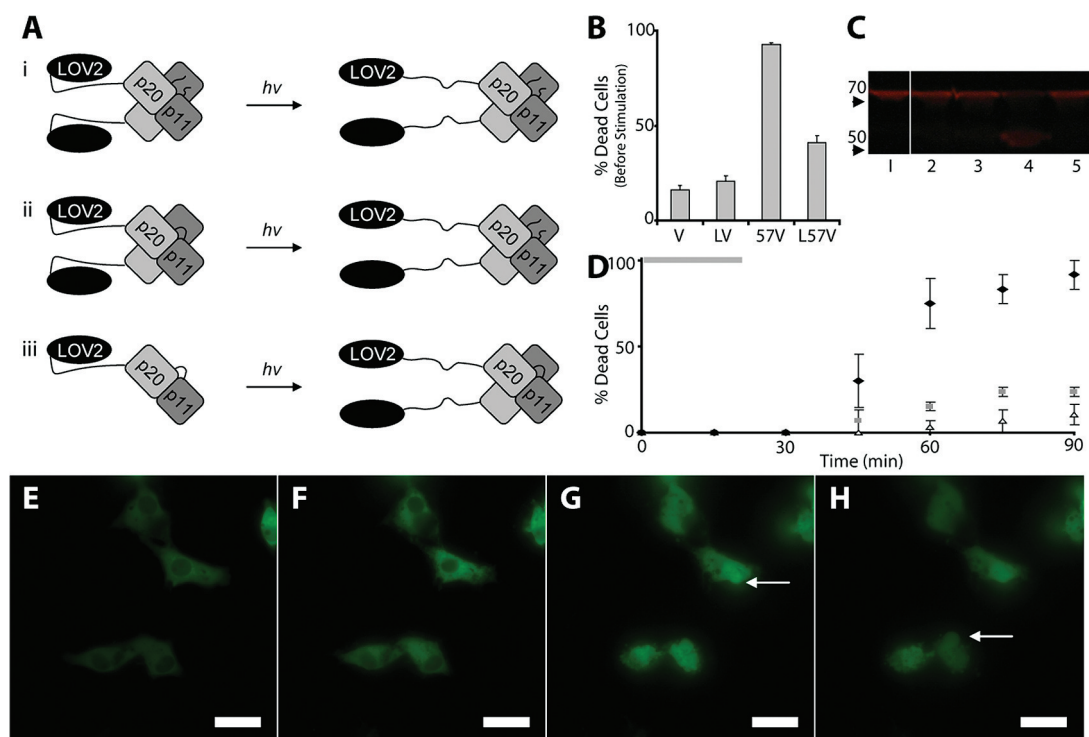


Figure 1. A photoactivated caspase-7 fusion protein. (A) Three potential mechanisms of photoactivation for L57V: allosteric (i), internal cleavage (ii) and dimerization (iii). (B) The percentage of dead cells 24 h after transfection and before illumination for Venus (V), LOV-Venus (LV), caspase57-303-V (57V), LOV-caspase57-303-V (L57V). (C) Fluorescent SDS-PAGE of *x*-DEVD-*y* incubated for 24 h with the following protein solutions: 1, itself; 2–4, L57V; 5, L57V(Cys186Ala). Samples 2–5 were exposed to blue light for 0, 2, 24, and 24 h, respectively. Mass markers are indicated to the left in kDa. (D) Time course showing the percentage of dead cells after illumination (illumination time indicated by gray bar) for L57V (black diamonds), LOV2-Venus (gray squares), and Venus (open triangles). (E–H) Images of cells 0, 30, 60, and 90 min after the start of the experiment. Arrows in panels E–H show plasma membrane blebs. Scale bars in panels E–H are 30 μ m. Error bars are the standard error; $n = 10$ experiments and over 100 observed cells for B; $n = 3$ experiments and over 10 observed cells for D. Images are false color.

fusions were made by truncating the catalytic domain of caspase-7 at different amino acids in the vicinity of the pro-domain cleavage site: at amino acids 52, 54, 56, 57, 58, and 60. Since the truncation mutant at amino acid 57 (named L57V) mediated blue light-induced cell death (as discussed below) more frequently than other mutants, it was chosen for further study (Supplemental Figures 1–3). Illumination causes unfolding of the LOV2 domain,¹⁰ which allows for caspase activity through the following possible mechanisms: change of dimerization state, allowance for internal cleavage, or allosteric activation (Figure 1A). Similar to the mechanism of other LOV2-based photoswitches,^{11,12} our evidence below suggests it is allosteric activation.

Caspase-7 Activity Is Suppressed When Fused with LOV2. The fusion of LOV2 to the catalytic domain of caspase-7 is able to suppress caspase-7 activity (Figure 1B). To test this we assayed the number of dead or dying transfected COS7 cells compared to the number of living transfected cells in a glass-bottom well (see Methods for more details). There was a significant reduction ($P < 0.001$) in the percentage of dead cells observed when L57V was expressed ($40.8 \pm 3.7\%$) compared to the catalytic domain, 57V, alone ($92.4 \pm 1.4\%$) (Figure 1B). This indicates that the fusion with the LOV2 domain was able to suppress the catalytic activity of caspase-7 in most cells. The suppression may be improved through LOV2 mutations that have been recently reported to stabilize LOV2 fusions.^{14b} Nevertheless, L57V in its current form routinely provided a large number of morphologically normal transfected cells with which to perform experiments.

L57V Mediates Blue Light-Induced Cell Death with Spatiotemporal Precision. L57V can cleave the caspase-7 substrate DEVD in a blue light-dependent manner *in vitro* (Figure 1C). A 70 kDa peptide was created of the form *x*-DEVD-*y* where *x* is a 15 kDa domain, *y* is a 55 kDa red fluorescent protein domain, and DEVD is a typical caspase-7 substrate (see Methods for more details). Solutions of L57V and *x*-DEVD-*y* were prepared and illuminated with blue light for 0, 2, and 24 h, as indicated. With 24 h of illumination *in vitro* there was a noticeable change in the migration of red fluorescence on SDS-PAGE, consistent with a reduction in size from 70 to 55 kDa (Figure 1C). There was no change in migration of red fluorescence when *x*-DEVD-*y* was incubated with a catalytically incompetent mutant of L57V.

COS7 cells expressing L57V and stimulated with blue light for 20 min began to show morphological changes consistent with apoptosis within 20–25 min after stimulation (Figure 1E–H). Cells were exposed to light (438 nm with a 24 nm bandpass from a xenon source) for an arbitrary duration of 20 min to stimulate undocking of the J α peptide from the LOV2 domain to release the active caspase domain. There were no apparent morphological changes in the first 10 min after stimulation (30 min total). However, within 20–25 min after stimulation (45 min total) many cells began to show morphological changes consistent with apoptosis including plasma membrane blebbing, condensation, and loss of nuclear envelope integrity (demonstrated by a loss in exclusion of the fluorescent construct from the nucleus). Over all trials $91.7 \pm 8.3\%$ of cells showed two or more morphological signs

suggestive of apoptosis within 70 min after stimulation (90 min total) (Figure 1D). Cells were observed using fluorescence and bright-field imaging to confirm that there were no apparent changes in subcellular localization or trafficking of L57V during cell death (Supplemental Figure 4).

Cells were observed for 90 min (70 min after the end of stimulation) because typically caspase-3/7 activation leads to cell rounding within 25–50 min¹⁶ and therefore changes to cells outside of this time frame are likely not related to the light stimulus. The apparent discord between illumination required time for *in vitro* DEVDase sensor cleavage (24 h), and presentation of cellular effects *in vivo* (90 min) is likely due to a combination of effects including substrate and sensor concentration, lack of feedback mechanisms *in vitro*, and a greater likelihood of poorly folded fusion proteins *in vitro*. The apparent expression level of L57V varied between cells, owing to gene delivery using transient transfection; however, we did not notice a stark relationship between expression (judged by fluorescence intensity) and efficiency of blue light-mediated morphology changes.

The light stimulation had little effect on cells transfected with control constructs (Venus or LOV2-Venus): only $10.4 \pm 8.3\%$ and $23.6 \pm 2.6\%$ of these cells showed morphological signs of death after stimulation, respectively (Figure 1D). This was most likely because of the thermal heating effects from the light source. Basic experiments were repeated in the HeLa cell line with very similar results, and we performed proof-of-principle studies showing blue light-induced cell death mediated by L57V in a variety of transformed cell lines including 3T3, HEK293, and CHO (Supplemental Figure 5).

Spatial control over L57V-mediated cell death is limited by the light source used for illumination (Figure 2). A field of COS7 cells expressing L57V was illuminated with light in only the center of the field for 20 min. Cells in the central part of the field showed marked morphological changes consistent with apoptosis, whereas cells outside the illuminated area were generally unchanged. This shows that L57V can potentially mediate cell death in a single cell or group of cells. There may be a small zone outside the illuminated area that is exposed to light scatter which may limit the spatial precision, but we have not observed this effect in any significant way.

There was an apparent threshold for stimulation (illumination time) below which there was little cell death and above which there was nearly complete cell death (Figure 3A,B). There was no significant difference between the percentage of cells showing death morphologies at 90 min after stimulations of 10, 20, or 30 min. Further, stimulation for 5 min was not significantly different than no stimulation at all (0 min). However, there was a significant ($P = 0.033$) difference between stimulations of 5 and 10 min (Figure 3A). This suggests that the minimum time for L57V activation to cause cell death is between 5 and 10 min.

L57V-Mediated Cell Death Is Dependent on Caspase-7 and LOV2 Domains. L57V-mediated cell death is caspase-dependent (Figure 3C). L57V-transfected cells preincubated with $100 \mu\text{M}$ *z*-DEVD-fmk caspase-3/7 inhibitor for 2 h showed minimal morphological changes that were not significantly different than stimulating Venus-transfected cells (Figure 3C, Supplemental Figure 6). To confirm the dependence of cell death on the caspase domain of L57V, the caspase domain was rendered catalytically incompetent (Cys186Ala),⁸ to produce dominant negative Ldn57V. There were no significant morphological differences between stimulated cells

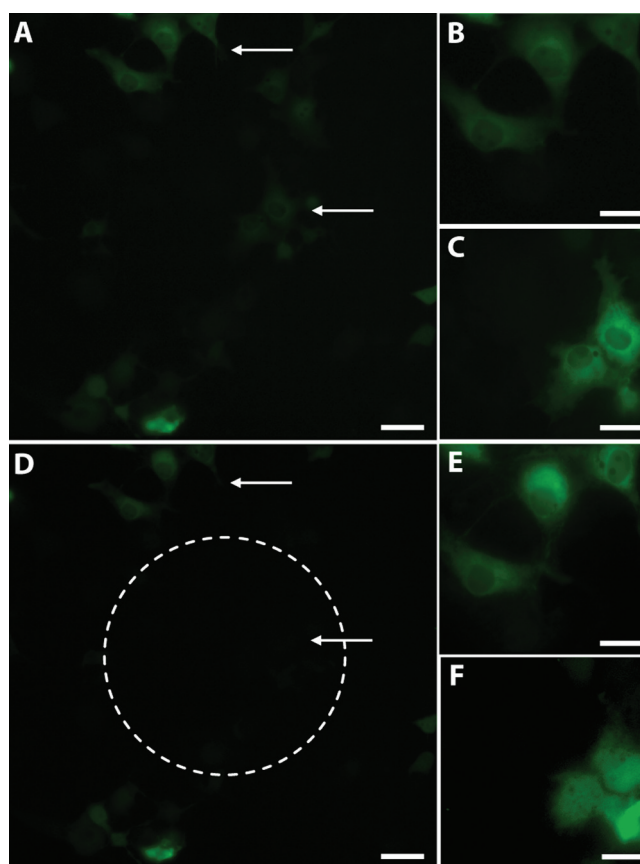


Figure 2. L57V-mediated death is spatially precise. (A) A low magnification (20 \times objective) image of COS7 cells expressing L57V, with two groups of cells identified by white arrows enlarged in panels B and C (60 \times objective). The center of the field was illuminated for 20 min. (D) The low magnification image of the same cells after 60 min shows that those within the illuminated zone (dotted white circle) have undergone significant morphological changes (and some photobleaching), whereas those outside the illuminated zone have changed very little. Again, two groups of cells identified by white arrows are enlarged in panels E and F. Scale bars are 50 μm in panels A and D and 30 μm in panels B, C, E, and F. Images are false color.

expressing Ldn57V and cells expressing Venus or a fusion of LOV2 and full length caspase-7, LfscaspV as controls (Figure 3C, Supplemental Figure 6). As well, cells co-expressing L57V and survivin, a 16 kDa inhibitor of apoptosis protein,¹⁷ showed minimal morphological changes that were not significantly different than control experiments (Figure 3C, Supplemental Figure 6).

As a further test of where L57V acts upon the apoptosis cascade, we co-transfected COS7 cells with a mRFP variant of L57V, L57-mRFP, and a plasmid encoding for Bcl-2.¹⁸ We hypothesized that overexpression of Bcl-2 would not disrupt L57V-mediated cell death because Bcl-2 is an upstream regulator of the caspase cascade. In cells expressing both Bcl-2 (fusion with Venus) and L57-mRFP, we noticed cells were much less likely to show signs of apoptosis than L57V alone ($P = 0.032$), and there was no significant difference between L57V + Bcl-2 and the Venus or LOV2-Venus controls (Figure 3C, Supplemental Figure 6). This was surprising to us because Bcl-2 is generally thought to inhibit apoptosis upstream of caspase-3/7.¹⁸ Given the role of Bcl-2 in inhibiting apoptosis through the mitochondrial pathway, this result may suggest that L57V, and perhaps caspase-3/7 in general, requires some contribution

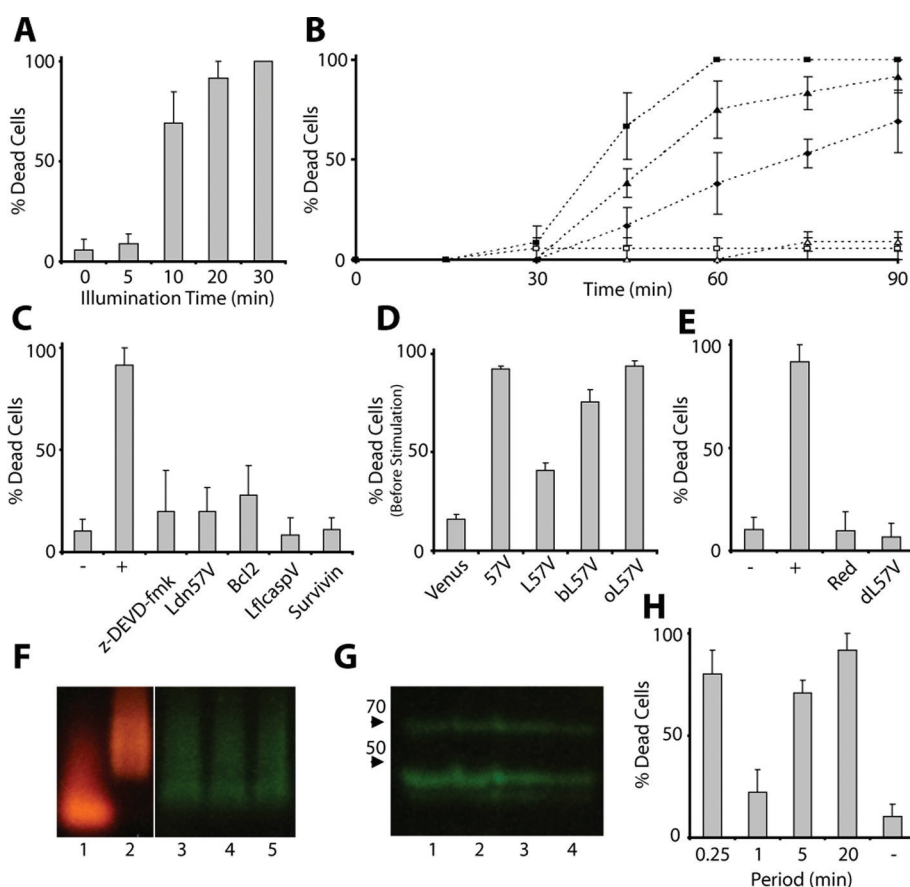


Figure 3. L57V mediates blue light-dependent cell death in stimulated COS7 cells. (A) The percentage of cells showing apoptosis-like morphologies 90 min after the start of stimulation, for the different illumination times indicated. (B) Time course showing the percentage of cells showing apoptosis-like morphologies for various illumination times. Filled squares, 30 min; filled triangles, 20 min; filled diamonds, 10 min; open triangles, 5 min; open squares, 0 min. (C, E, H) The percentage of cells showing apoptosis-like morphologies 90 min after the start of stimulation for the different conditions indicated. (D) The percentage of apoptotic-like cells observed in glass dishes prior to imaging for the given transfected constructs. The control data is reproduced from Figure 1B. (F) Fluorescent Native-PAGE of protein solutions: 1, mRFP; 2, dsRed, 3–5, L57V exposed to blue light for 0, 2, and 24 h, respectively. (G) Fluorescent SDS-PAGE of L57V exposed to blue light for (1) 0 h, (2) 2 h, (3) 24 h, and (4) 48 h. The molecular mass on the left is indicated in kDa. Error bars are the standard error; $n = 10$ experiments and over 100 observed cells for D; $n = 3$ experiments and over 10 observed cells for A–C, E, H. “–” denotes cell death with Venus transfected, “+” denotes cell death with L57V transfected, and these are the same data used throughout the figure.

from the mitochondrial portion of the apoptosis cascade in order for the cell to fully commit itself to apoptosis.¹⁹ However, the precise role of Bcl-2 here is unclear given that Bcl-2 overexpression has also been shown to prevent caspase-independent forms of apoptosis.²⁰

L57V-mediated cell death is dependent on blue light activation of the LOV2 domain (Figure 3D–F). Two mutations have been reported for LOV2 that promote undocking of the $J\alpha$ peptide (Ile539Glu) or render LOV2 insensitive to blue light (Cys450Met).^{10,21} We refer to these mutations throughout as “bright” LOV and “dark” LOV, since they mimic the effects of illumination and darkness, respectively. The bright L57V mutant, bL57V, caused a high rate of death in transfected cells before illumination ($75.7 \pm 6.1\%$) that was significantly higher than L57V ($P < 0.001$) but less than 57V ($P = 0.017$) (Figure 3D). We suspected that LOV2 was only partially unfolded in bL57V, since it has not been conclusively established in the literature that Ile539Glu fully opens LOV2 in the dark.²¹ We created a fully open mutant of LOV2 using the TEV substrate peptide ENLYFQS²² (Supplemental Figure 7) and made an open L57V, or oL57V. As expected, oL57V had nearly all transfected cells dead before illumination ($93.7 \pm$

2.7%), which was not significantly different than 57V. The dark L57V mutant, dL57V, did not mediate blue light-induced cell death, and cells expressing dL57V were not significantly different than control cells expressing Venus (Figure 3E).

Additional experiments were highly suggestive of the light-induced unfolding model of L57V activation (Figure 3E–H): illumination with red-yellow light, which does not activate LOV2,^{10b} did not cause cell death beyond the control experiments (Figure 3E). L57V solutions were prepared *in vitro*, illuminated for 0, 2, or 24 h, and visualized using fluorescent Native-PAGE (Figure 3F). Illumination had no effect on the apparent size of L57V on Native-PAGE, suggesting that illumination does not alter the dimerization state and that changes in dimerization are not involved in blue light activation of L57V. This experiment does not directly comment on whether L57V is a monomer or dimer in the dark state, but it is known that the caspase zymogen exists as a dimer^{6c} and so L57V is also likely a dimer in the dark state. As a positive control we showed that there is a difference in the apparent size of mRFP and dsRed, two red fluorescent proteins known to exist in different oligomerization states (monomer for mRFP and tetramer for dsRed).²³ Illumination also had no

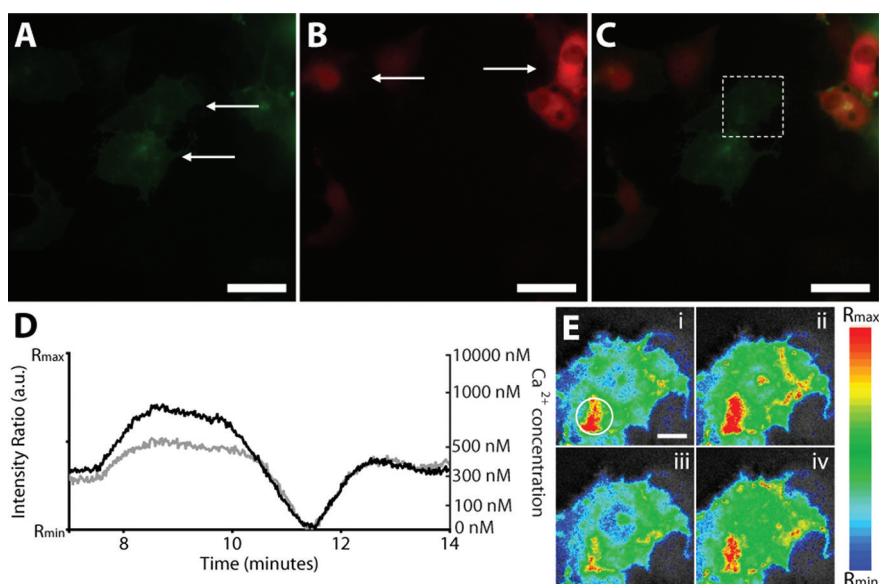


Figure 4. ATP release from apoptotic cells monitored by the P2X2 channel and a Ca^{2+} FRET biosensor. COS7 cells transfected with LS7-mRFP are co-cultured with COS7 cells co-transfected with a membrane-targetted YFP/CFP Ca^{2+} biosensor and P2X2-CFP. (A) YFP image before stimulation showing two cells that will act as the ATP sensors (white arrows). (B) RFP image before stimulation showing cells that act as ATP sources (white arrows). (C) Merged image of panels A and B showing the spatial relationship between ATP sensors and sources. Cells that are triple co-transfected are not used as ATP sensors. The region enlarged in panel E is highlighted with a dashed white box. (D) Plot of the intensity ratios for the Ca^{2+} biosensor versus time after the 20 min illumination period. The black plot is from the ROI indicated by a white circle in panel E.i, and the gray plot is of the entire cell for comparison. (E) Magnified images of one of the ATP sensor cells with a blue to red mask to show spatial changes in the FRET efficiency ratio. Scale bars in A–C are $30 \mu\text{m}$, and scale bar in E is $7.5 \mu\text{m}$. Images are false color.

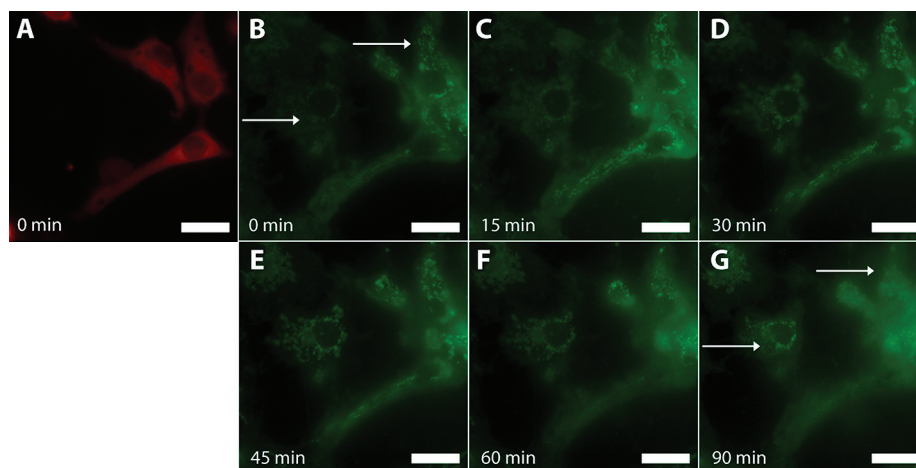


Figure 5. Mitochondrial dysfunction in LS7V-transfected cells. (A) COS7 cells transfected with LS7-mRFP are shown before stimulation. (B) Transfected and nontransfected neighbors are preincubated with MitoSensor reagent for 0.5 h before stimulation. In both types of cells the fluorescence is well localized to mitochondria (white arrows). (C–G) After 20 min of light stimulation, MitoSensor translocates from mitochondria to cytoplasm in transfected cells, indicating mitochondrial dysfunction. In nontransfected cells the dye distribution at 90 min is very similar to the distribution before stimulation (white arrows). Scale bars in all images are $30 \mu\text{m}$.

effect on the apparent proportion of cleaved subunit to uncleaved, full length LS7V detected through SDS-PAGE after 0, 2, 24, and 48 h of light exposure (Figure 3G). This suggests that internal caspase cleavage is not significantly affected by LOV2 unfolding.

As a further test, LS7V-expressing cells were exposed to oscillating light pulses with different periods, T , for n cycles, subject to $T \cdot n = 20$ min with 50% duty cycle (Figure 3H). For example, for experiments with period $T = 1$ min, cells were exposed to 1 min of light, then 1 min of darkness for 40 min such that total illumination time was still 20 min. Consistent

with our theory that LS7V must be activated for 5–10 min to cause cell death, when $T = 5$ min, cell death occurred frequently ($70.8 \pm 6.3\%$), whereas when $T = 1$ min, cell death was uncommon ($22.2 \pm 11.1\%$) (Figure 3H). We suspected that oscillations faster than the thermal relaxation time of LOV2, about 0.5 min,²⁴ would mimic the effect of constant illumination and result in extensive cell death. Indeed, when $T = 0.25$ min, cell death occurred in $80.0 \pm 11.5\%$ of cases (Figure 3H). These results can only be explained by assuming the unfolding of the LOV2 domain of LS7V releases inhibition on the catalytic domain.

L57V-Mediated Cell Death Is Apoptosis. L57V-mediated cell death is apoptosis (Figures 4 and 5; Supplemental Figures 8 and 9). Several biochemical signatures of apoptosis have been identified during L57V-mediated cell death including ATP release, mitochondrial dysfunction, and translocation of a caspase-specific biosensor. Morphological characteristics (Figure 1) and caspase dependence (Figure 3) are highly suggestive of apoptosis, but further confirmation is important to verify the mode of cell death. Not all conventional tests for apoptosis are appropriate here (e.g., TUNEL assay) because live-cell imaging restricts the ability to manipulate the sample during observation.

ATP release is a specific feature of apoptotic cell death that is thought to act as a signal for cell clearance by phagocytic cells of the immune system.² We co-cultured COS7 cells expressing L57-mRFP (a mRFP variant of L57V) with COS7 cells expressing a FRET-based Ca^{2+} biosensor²⁵ and the ATP-sensitive P2X2 channel.²⁶ The biosensor was fused with a lipid raft-targeting peptide²⁷ to further amplify any detected signal at the cell membrane (Supplemental Figure 8). A Ca^{2+} transient typical of P2X2 activation was observed 5–10 min after the 20 min illumination period (Figure 4) in approximately 50% of experiments conducted (5/9 independent experiments). The hyperpolarization period was characteristic of P2X2 activation by ATP²⁸ and the spatial localization of the Ca^{2+} transient within the cell was correlated with the subcellular localization of the biosensor. The release of ATP by stimulated L57V-expressing cells is significant because it shows that at least one of the natural communication mechanisms between apoptotic cells and their environment is unaltered. This creates the potential to develop more complex systems whereby newly apoptotic cells can communicate and affect their neighbors in a predictable way. This system may also be used to provide insights into the physiological role of ATP release by cells early in apoptosis.

Further experiments with two distinct probes confirmed apoptotic cell death. First, experiments with MitoSensor reagent showed that the mitochondrial membrane potential was normal in morphologically normal, unstimulated L57-mRFP cells (Figure 5). Within 10 min after stimulation (30 min total) the MitoSensor reagent began to translocate into the cytoplasm, which is consistent with a loss of mitochondrial membrane potential and apoptosis,²⁹ and the translocation was complete within 40 min after stimulation. Importantly, there was no translocation of MitoSensor in neighboring cells that were not transfected with L57-mRFP (Figure 5), which further shows the potential for precise spatial control over L57V-mediated cell death.

Second, COS7 cells were co-transfected with L57-mRFP and a caspase-3/7 specific biosensor that translocates from the plasma membrane to the nucleus after caspase cleavage. We observed translocation of this biosensor within 10–15 min after the onset of illumination (Supplemental Figure 9). The biosensor, based on previous designs,³⁰ used YFP and CFP and so L57-mRFP was used to mediate cell death. This timeline is consistent with the earlier results that there is a threshold for illumination of 5–10 min before L57V is capable of causing cell death. A nuclear-translocating biosensor has the advantage over a FRET-based sensor of observing two stages of cell death: initial cleavage and nuclear envelope breakdown. Initial cleavage causes fluorescence to localize to the nucleus, and when the nuclear envelope loses integrity, the translocating fragment of the biosensor diffuses into the cytoplasm

(Supplemental Figure 9). This second event occurred simultaneously with RFP diffusion into the nucleus. The relative dimness of the CFP channel initially is due to FRET between the translocating CFP and membrane-tethered YFP. Partial photobleaching of CFP during LOV2 illumination prevents the signal from increasing in intensity after translocation. The extent of translocation was quantified by calculating the Pearson's correlation coefficient between CFP and YFP (a decrease in correlation was observed around 15–30 min, consistent with DEVDase activity in that time frame) and CFP and RFP (an initially low correlation was observed while CFP is imported to the nucleus and RFP is excluded by size; the correlation increases slightly when both signals become diffusely cytoplasmic after NEB). A catalytically incompetent mutant (Cys186Ala, or Ldn57-mRFP) was used as a negative control with the DEVDase sensor (Supplemental Figure 9; details in Methods). Taken together, these results confirm that apoptosis is the mode of cell death induced by blue light stimulation of cells expressing L57V.

We have created a synthetic protein (L57V) that transduces a light input into a cell death signal by fusing the LOV2 domain from phototropin1 with the catalytic domain of caspase-7. Our evidence suggests that the mechanism used by L57V to activate caspase-7 is allosteric as light does not change the dimerization state. Furthermore, the photoactivity of L57V is very sensitive to the point of fusion between the LOV2 domain and the catalytic domain of caspase-7. Two lines of evidence suggest that L57V begins to substantially cleave caspase-7 targets after 5–10 min of stimulation. This suggests that these cells are tolerant to some degree of transient caspase-7 activation, which may not be surprising given the apoptosis cascade is highly regulated from initiation to execution. This type of temporal insight into the apoptosis cascade is possible using genetically targeted, photoactivated proteins.

Many characteristics of apoptosis that we have observed (such as mitochondrial dysfunction, ATP release, and morphological changes) occur much later and nearly always after the light stimulation has ended. This suggests that L57V cleaves targets within the cell (likely other caspases such as caspase-9³¹) that begin the apoptosis program in earnest, rather than L57V directly executing apoptosis. This “feedback” notion is present in the literature^{22,31} but difficult to study in living cells given the currently available tools. However, it is consistent with our observation that overexpression of proteins typically thought to act upstream of caspase-7 (such as Bcl-2) can inhibit L57V-mediated cell death. These points suggest that a cell's “decision” to undergo apoptosis is complex and cannot be simplified to considering the activation state of a single protein.

L57V-mediated cell death is spatially and temporally well-defined, and a non-laser source is sufficient stimulation. Consequently, the affect of apoptosis in a particular space, or on a particular subset of cells, can be studied in the context of a multicellular environment without significant damage to nonexpressing cells. Particular avenues for further research may include cell clearance studies where L57V is used to initiate apoptosis and clearance signals, neuronal mapping by loss-of-function induced by L57V, or further studies into the biochemical signatures of apoptosis in a variety of cell configurations and environments where small molecule inducers (such as staurosporine, or the recently reported rapamycin-inducible caspase system³²) are not appropriate. The dynamic range and activation characteristics of L57V may be

improved using a variety of techniques including rationally designed mutations to LOV2 that have recently been reported to improve LOV2 photoswitches^{14b} or by applying the LOV2 fusion to structurally similar caspases.

Caspase-dependent apoptosis is a conserved cell death program involved in physiological development and numerous pathological states ranging from cancer to HIV/AIDS. Herein we have developed a photoactivated protein switch that can specifically activate the executioner caspase-7 in response to blue light. The ability to activate the apoptotic cascade with temporal accuracy at a specific node of the cascade will facilitate further study of the protein–protein interactions involved in executing apoptosis. In particular, the characterization of L57V presented here demonstrates that feedback mechanisms and inherent tolerances of a cell to caspase-7 and the full execution of apoptosis can be studied at the single-cell level. In contrast to the recently reported small molecule-activated caspase-3, activation of apoptosis with spatial precision, limited by the light source used, was demonstrated. Thus L57V could be used to conduct cell ablation studies such as neuronal mapping or wound repair. A photoactivated apoptosis trigger may also find utility in the context of gene therapy, whereby L57V could be delivered to diseased cells to promote spatiotemporally controlled death *in vivo*. Finally, the design and characterization of L57V adds to the growing collection of photoactivated protein switches based on LOV2, including PARac, LovTAP, and LOVSIK, further establishing LOV2 as an exceptionally useful component in the toolbox of protein engineers.

METHODS

Complete methods are available in the Supporting Information.

Plasmids. All peptides used were inserted to pCfVtx3³³ after PCR from plasmid or cDNA sources. LOV2 and Bcl-2 were from Addgene (Cambridge, MA) plasmids 22027 and 8793, respectively. The caspase catalytic domain was amplified from human cDNA.

Cell Culture and Transfection. COS7 and HeLa cells were maintained in Dulbecco's Modified Eagle's Medium supplemented with 25 mM D-glucose, 1 mM sodium pyruvate, and 4 mM L-glutamine (Invitrogen, Carlsbad, CA) in a T25 flask. Cells were passaged at 95% confluency using 0.05% trypsin with EDTA (Sigma Aldrich, St. Louis, MO) and seeded onto glass-bottom dishes at 1:15 dilution (Mattek, Ashland, MA). Cells were transiently transfected using Lipofectamine 2000 according to manufacturer's directions (Invitrogen).

Illumination and Imaging. Imaging was performed using an inverted IX81 microscope with Lambda DG4 xenon lamp source and QuantEM 512SC CCD camera (Olympus, Markham, ON, Canada). Filter excitation (EX) and emission (EM) bandpass specifications were as follows (in nm): for CFP EX 438/24, EM 482/32; for YFP EX 500/24, EM 542/27; for RFP EX 580/20, EM 630/60 (Semrock, Rochester, NY, USA). For LOV2, excitation was using the CFP excitation filter, and the RFP excitation filter for the "red" experiments. The light intensity was 25 mW/cm².

Statistical Analysis. For light-stimulation experiments, data is presented as the mean \pm standard error of at least three independent experiments that included at least 10 cells. For cell viability before light-stimulation experiments, data are presented as the mean \pm standard error of at least 10 independent experiments that included at least 100 cells. Significance between conditions was calculated using the Student's *t* test and *P* < 0.05 were considered significant.

ASSOCIATED CONTENT

Supporting Information

This material is available free of charge *via* the Internet at <http://pubs.acs.org>.

AUTHOR INFORMATION

Corresponding Author

*Tel: 416-978-7772. Fax: 416-978-4317. E-mail: kevin.truong@utoronto.ca.

Author Contributions

E.M. designed and carried out most experiments, analyzed the data, and wrote the manuscript. X.C. created the caspase biosensor and helped write the manuscript. E.P. and S.W. produced plasmids used in the work. K.T. conceived the initial idea, analyzed the data, and helped write the manuscript.

Notes

The authors declare no competing financial interests.

ACKNOWLEDGMENTS

This work was made possible by plasmid sharing through Addgene, particularly by K. M. Hahn for depositing PA-Rac. This work was supported by fellowships to E.M. and E.P. from the Natural Science and Engineering Research Council (NSERC) and a grant to K.T. from the Canadian Institutes of Health Research (no. 81262).

REFERENCES

- (1) Jacobson, M. D., Weil, M., and Raff, M. C. (1997) Programmed cell death in animal development. *Cell* 88 (3), 347–54.
- (2) Elliott, M. R., Chekeni, F. B., Trampont, P. C., Lazarowski, E. R., Kadl, A., Walk, S. F., Park, D., Woodson, R. I., Ostankovich, M., Sharma, P., Lysiak, J. J., Harden, T. K., Leitinger, N., and Ravichandran, K. S. (2009) Nucleotides released by apoptotic cells act as a find-me signal to promote phagocytic clearance. *Nature* 461 (7261), 282–6.
- (3) Vaux, D. L., and Flavell, R. A. (2000) Apoptosis genes and autoimmunity. *Curr. Opin. Immunol.* 12 (6), 719–24.
- (4) Hanahan, D., and Weinberg, R. A. (2000) The hallmarks of cancer. *Cell* 100 (1), 57–70.
- (5) Gougeon, M. L., and Piacentini, M. (2009) New insights on the role of apoptosis and autophagy in HIV pathogenesis. *Apoptosis* 14 (4), 501–8.
- (6) (a) Mashima, T., Naito, M., and Tsuruo, T. (1999) Caspase-mediated cleavage of cytoskeletal actin plays a positive role in the process of morphological apoptosis. *Oncogene* 18 (15), 2423–30. (b) Kramer, A., Liashkovich, I., Oberleithner, H., Ludwig, S., Mazur, I., and Shahin, V. (2008) Apoptosis leads to a degradation of vital components of active nuclear transport and a dissociation of the nuclear lamina. *Proc. Natl. Acad. Sci. U.S.A.* 105 (32), 11236–41. (c) Riedl, S. J., Fuentes-Prior, P., Renatus, M., Kairies, N., Krapp, S., Huber, R., Salvesen, G. S., and Bode, W. (2001) Structural basis for the activation of human procaspase-7. *Proc. Natl. Acad. Sci. U.S.A.* 98 (26), 14790–5.
- (7) Riedl, S. J., and Shi, Y. (2004) Molecular mechanisms of caspase regulation during apoptosis. *Nat. Rev. Mol. Cell Biol.* 5 (11), 897–907.
- (8) Shi, Y. (2002) Mechanisms of caspase activation and inhibition during apoptosis. *Mol. Cell* 9 (3), 459–70.
- (9) Klaiman, G., Champagne, N., and LeBlanc, A. C. (2009) Self-activation of Caspase-6 *in vitro* and *in vivo*: Caspase-6 activation does not induce cell death in HEK293T cells. *Biochim. Biophys. Acta* 1793 (3), 592–601.
- (10) (a) Harper, S. M., Neil, L. C., and Gardner, K. H. (2003) Structural basis of a phototropin light switch. *Science* 301 (5639), 1541–4. (b) Salomon, M., Christie, J. M., Knieb, E., Lempert, U., and Briggs, W. R. (2000) Photochemical and mutational analysis of the

FMN-binding domains of the plant blue light receptor, phototropin. *Biochemistry* 39 (31), 9401–10.

(11) Wu, Y. L., Frey, D., Lungu, O. I., Jaehrig, A., Schlichting, I., Kuhlman, B., and Hahn, K. M. (2009) A genetically encoded photoactivatable Rac controls the motility of living cells. *Nature* 461 (7260), 104–8.

(12) Strickland, D., Moffat, K., and Sosnick, T. R. (2008) Light-activated DNA binding in a designed allosteric protein. *Proc. Natl. Acad. Sci. U.S.A.* 105 (31), 10709–14.

(13) Pham, E., Mills, E., and Truong, K. (2011) A synthetic photoactivated protein to generate local or global Ca^{2+} signals. *Chem. Biol.* 18 (7), 880–90.

(14) (a) Lee, J., Natarajan, M., Nashine, V. C., Socolich, M., Vo, T., Russ, W. P., Benkovic, S. J., and Ranganathan, R. (2008) Surface sites for engineering allosteric control in proteins. *Science* 322 (5900), 438–42. (b) Strickland, D., Yao, X., Gawlak, G., Rosen, M. K., Gardner, K. H., and Sosnick, T. R. (2010) Rationally improving LOV domain-based photoswitches. *Nat. Methods* 7 (8), 623–6.

(15) Rekas, A., Alattia, J. R., Nagai, T., Miyawaki, A., and Ikura, M. (2002) Crystal structure of venus, a yellow fluorescent protein with improved maturation and reduced environmental sensitivity. *J. Biol. Chem.* 277 (52), 50573–8.

(16) Chiang, J. J., and Truong, K. (2005) Using co-cultures expressing fluorescence resonance energy transfer based protein biosensors to simultaneously image caspase-3 and Ca^{2+} signaling. *Biotechnol. Lett.* 27 (16), 1219–27.

(17) Shin, S., Sung, B. J., Cho, Y. S., Kim, H. J., Ha, N. C., Hwang, J. I., Chung, C. W., Jung, Y. K., and Oh, B. H. (2001) An anti-apoptotic protein human survivin is a direct inhibitor of caspase-3 and -7. *Biochemistry* 40 (4), 1117–23.

(18) Chipuk, J. E., Moldoveanu, T., Llambi, F., Parsons, M. J., and Green, D. R. (2010) The BCL-2 family reunion. *Mol. Cell* 37 (3), 299–310.

(19) Ricci, J. E., Gottlieb, R. A., and Green, D. R. (2003) Caspase-mediated loss of mitochondrial function and generation of reactive oxygen species during apoptosis. *J. Cell Biol.* 160 (1), 65–75.

(20) Jung, K. C., Park, W. S., Kim, H. J., Choi, E. Y., Kook, M. C., Lee, H. W., and Bae, Y. (2004) TCR-independent and caspase-independent apoptosis of murine thymocytes by CD24 cross-linking. *J. Immunol.* 172 (2), 795–802.

(21) Harper, S. M., Christie, J. M., and Gardner, K. H. (2004) Disruption of the LOV-Jalpha helix interaction activates phototropin kinase activity. *Biochemistry* 43 (51), 16184–92.

(22) Phan, J., Zdanov, A., Evdokimov, A. G., Tropea, J. E., Peters, H. K. 3rd, Kapust, R. B., Li, M., Wlodawer, A., and Waugh, D. S. (2002) Structural basis for the substrate specificity of tobacco etch virus protease. *J. Biol. Chem.* 277 (52), 50564–72.

(23) Wall, M. A., Socolich, M., and Ranganathan, R. (2000) The structural basis for red fluorescence in the tetrameric GFP homolog DsRed. *Nat. Struct. Biol.* 7 (12), 1133–8.

(24) Chen, E., Swartz, T. E., Bogomolni, R. A., and Kliger, D. S. (2007) A LOV story: the signaling state of the phot1 LOV2 photocycle involves chromophore-triggered protein structure relaxation, as probed by far-UV time-resolved optical rotatory dispersion spectroscopy. *Biochemistry* 46 (15), 4619–24.

(25) Mank, M., Reiff, D. F., Heim, N., Friedrich, M. W., Borst, A., and Griesbeck, O. (2006) A FRET-based calcium biosensor with fast signal kinetics and high fluorescence change. *Biophys. J.* 90 (5), 1790–6.

(26) Khakh, B. S., Fisher, J. A., Nashmi, R., Bowser, D. N., and Lester, H. A. (2005) An angstrom scale interaction between plasma membrane ATP-gated P2X2 and alpha4beta2 nicotinic channels measured with fluorescence resonance energy transfer and total internal reflection fluorescence microscopy. *J. Neurosci.* 25 (29), 6911–20.

(27) Inoue, T., Heo, W. D., Grimley, J. S., Wandless, T. J., and Meyer, T. (2005) An inducible translocation strategy to rapidly activate and inhibit small GTPase signaling pathways. *Nat. Methods* 2 (6), 415–8.

(28) Fujiwara, Y., and Kubo, Y. (2006) Regulation of the desensitization and ion selectivity of ATP-gated P2X2 channels by phosphoinositides. *J. Physiol.* 576 (Pt 1), 135–49.

(29) Wang, X. (2001) The expanding role of mitochondria in apoptosis. *Genes Dev.* 15 (22), 2922–33.

(30) Bardet, P. L., Kolahgar, G., Mynett, A., Miguel-Aliaga, I., Briscoe, J., Meier, P., and Vincent, J. P. (2008) A fluorescent reporter of caspase activity for live imaging. *Proc. Natl. Acad. Sci. U.S.A.* 105 (37), 13901–5.

(31) Zou, H., Yang, R., Hao, J., Wang, J., Sun, C., Fesik, S. W., Wu, J. C., Tomaselli, K. J., and Armstrong, R. C. (2003) Regulation of the Apaf-1/caspase-9 apoptosome by caspase-3 and XIAP. *J. Biol. Chem.* 278 (10), 8091–8.

(32) Gray, D. C., Mahrus, S., and Wells, J. A. (2010) Activation of specific apoptotic caspases with an engineered small-molecule-activated protease. *Cell* 142 (4), 637–46.

(33) Truong, K., Khorchid, A., and Ikura, M. (2003) A fluorescent cassette-based strategy for engineering multiple domain fusion proteins. *BMC Biotechnol.* 3, 8.